10. L. M. Futey, Q. G. Medley, G. P. Cote, T. T. Egelhoff, *J. Biol. Chem.* **270**, 523 (1995).
11. A. G. Ryazanov *et al.*, *Proc. Natl. Acad. Sci. U.S.A.* **94**, 4884 (1997).
12. A. G. Ryazanov, K. S. Pavur, M. V. Dorovkov, *Curr. Biol.* **9**, R43 (1999).
13. Single-letter abbreviations for the amino acid residues are as follows: A, Ala; C, Cys; D, Asp; E, Glu; F, Phe; G, Gly; H, His; I, Ile; K, Lys; L, Leu; M, Met; N, Asn; P, Pro; Q, Gln; R, Arg; S, Ser; T, Thr; V, Val; W, Trp; and Y, Tyr.
14. H. Stenmark, R. Aasland, B. H. Toh, A. D'Arrigo, *J. Biol. Chem.* **271**, 24048 (1996).
15. T. A. Diggle, C. K. Seehra, S. Hase, N. T. Redpath, *FEBS Lett.* **457**, 189 (1999).
16. Phosphorylation reactions containing purified GST-kinase fusion proteins and mutants were incubated at 37°C for 30 min in the presence or absence of MBP as a test substrate in a 50-μl reaction. These reactions were performed in KIN buffer {50 mM Mops (pH 7.2), 100 mM NaCl, 20 mM $MgCl_2$, 0.5 mM ATP, and 2 μCi of [γ-^{32}P]ATP}. Immunokinase reactions containing immunopurified TRP-PLIK-HA (*8*) were incubated at 37°C for 30 min in a 50-μl reaction containing KIN buffer with 75 mM *n*-octyl-β-D-glucopyranoside. The reactions were terminated by the addition of 2× SDS sample buffer, and the proteins were resolved by SDS-PAGE and Coomassie staining for the GST-kinase experiment or by SDS-PAGE and Western blotting for the immunokinase assay. The gels were dried, and ^{32}P incorporation was visualized by autoradiography for the GST-kinase experiment. For the immunokinase experiment, ^{32}P incorporation was visualized by autoradiography of the transferred proteins on polyvinylidene difluoride membrane (Bio-Rad) before Western blotting.
17. S. K. Hanks, T. Hunter, *FASEB J.* **9**, 576 (1995).
18. S. Misra, J. H. Hurley, *Cell* **97**, 657 (1999).
19. The TRP-PLIK clone in the pTracerCMV2 (Invitrogen) vector was transiently transfected with LipofectAMINE 2000 (Gibco). Cells were transferred to cover slips 12 hours after transfection, and electrophysiological measurements were made 24 hours after transfection (22 ± 2°C). The TRP-PLIK–expressing CHO-K1 cells were detected by GFP fluorescence. Membrane currents were digitized at 10 or 20 kHz and digitally filtered off line at 1 kHz. Voltage stimuli lasting 500 ms were delivered at 5-s intervals, with either voltage ramps or voltage steps from −100 to +100 mV. The internal pipette solution for macroscopic and single-channel currents contained 145 mM Cs-methanesulfonate, 8 mM NaCl, 5 mM ATP, 1 mM $MgCl_2$, 10 mM EGTA, 4.1 mM $CaCl_2$, and 10 mM Hepes, with pH adjusted to 7.2 with CsOH after addition of ATP. The standard extracellular solution contained 140 mM NaCl, 5 mM CsCl, 2.8 mM KCl, 2 mM $CaCl_2$, 1 mM $MgCl_2$, 10 mM Hepes, and 10 mM glucose, with pH adjusted to 7.4 with NaOH. Relative ion permeabilities were measured with the pipette solution containing 145 mM Cs-methanesulfonate, 10 mM CsCl, 5 mM ATP, 10 mM EGTA, and 10 mM Hepes (pH 7.2) and the external solution containing 110 mM $NMDG^+$, 30 mM X^+ (Na^+, Ca^{2+}, K^+, or Cs^+), 10 mM Hepes, and 10 mM glucose (pH 7.4). The relative permeability for monovalent ions was calculated according to the equation $P_X/P_{Cs} = ([Cs^+]_o/[X^+]_o)\exp[F(E_X - E_{Cs})/RT]$. The P_{Ca}/P_{Cs} permeability ratio was calculated according to the equation $P_{Ca}/P_{Cs} = \{[Cs^+]_o\exp(-FE_{Cs}/RT)\exp(FE_{Ca}/RT)[\exp(FE_{Ca}/RT)+1]\}/(4[Ca^{2+}]_o)$, where R, T, and F are the gas constant, absolute temperature, and Faraday's constant, respectively. Statistical comparisons were made with the two-way analysis of variance (ANOVA) and two-tailed t test with Bonferroni correction; $P < 0.05$ indicated statistical significance.
20. I. B. Levitan, *Adv. Second Messenger Phosphoprotein Res.* **33**, 3(1999).
21. G. Yellen, *Q. Rev. Biophys.* **31**, 239 (1998).
22. Supplementary data are available at www.sciencemag.org/cgi/content/full/1058519/DC1.

21 December 2000; accepted 9 January 2001
Published online 18 January 2001;
10.1126/science.1058519
Include this information when citing this paper.

REPORTS

Role of the ENTH Domain in Phosphatidylinositol-4,5-Bisphosphate Binding and Endocytosis

Toshiki Itoh,[1] Seizo Koshiba,[2] Takanori Kigawa,[2,3] Akira Kikuchi,[4] Shigeyuki Yokoyama,[2,3,5] Tadaomi Takenawa[1]*

Endocytic proteins such as epsin, AP180, and Hip1R (Sla2p) share a conserved modular region termed the epsin NH_2-terminal homology (ENTH) domain, which plays a crucial role in clathrin-mediated endocytosis through an unknown target. Here, we demonstrate a strong affinity of the ENTH domain for phosphatidylinositol-4,5-bisphosphate [PtdIns(4,5)P_2]. With nuclear magnetic resonance analysis of the epsin ENTH domain, we determined that a cleft formed with positively charged residues contributed to phosphoinositide binding. Overexpression of a mutant, epsin Lys^{76} → Ala^{76}, with an ENTH domain defective in phosphoinositide binding, blocked epidermal growth factor internalization in COS-7 cells. Thus, interaction between the ENTH domain and PtdIns(4,5)P_2 is essential for endocytosis mediated by clathrin-coated pits.

ENTH domains are structural modules of ~140 amino acids found in mammalian epsin 1 and 2, AP180, and Hip1R, as well as in their yeast homologs, Ent1p through Ent4p, yAP180, and Sla2p (*1–4*). Mammalian epsin plays a crucial role in clathrin-mediated endocytosis (*2*). Yeast Ent1p and Ent2p are essential for actin function and for endocytosis. Disruption of both genes in yeast is lethal, and the ENTH domain is required to inhibit lethality. Almost all temperature-sensitive alleles of the ENT1 gene are found within the ENTH domain, supporting its importance (*3*). The essential function of the conserved ENTH domain from yeast to mammal prompted us to identify its downstream target. Using an ENTH affinity chromatography column, we were not able to detect any protein from bovine brain extract bound to the epsin ENTH domain. Because clathrin-mediated endocytosis is mediated by a specific interaction between endocytic proteins and the lipid bilayer to form invaginated buds and coated vesicles (*5*, *6*), and because many biochemical and physiological studies suggest important roles for phosphoinositides in endocytosis and vesicular trafficking (*7–9*), we examined the possibility that the ENTH domain binds to phosphoinositides.

To determine whether the ENTH domain could bind phosphoinositides, we subjected a glutathione *S*-transferase (GST) fusion protein of the epsin ENTH domain to liposome binding assay. Although epsin ENTH did not co-sediment with phosphatidylethanolamine (PE)– and phosphatidylcholine (PC)–based liposomes, increasing concentrations of phosphatidylinositol4,5-bisphosphate [PtdIns(4,5)P_2] in the liposomes resulted in co-sedimentation of the ENTH domain (Fig. 1A). Co-sedimentation was not observed in the presence of increased concentrations of PtdIns in the liposomes, demonstrating a high specificity for the interaction with PtdIns(4,5)P_2. Co-sedimentation was clearly observed at 0.2% PtdIns(4,5)P_2, and the dissociation constant K_d for the interaction was estimated at 0.37 μM. The strong interaction between the ENTH domain and PtdIns(4,5)P_2 was confirmed by other methods, including overlay assays with protein probe against phospholipids (Fig. 1B) and lipid probe against the ENTH domain blotted onto nitrocellulose membrane (Fig. 1C). The specificity of the binding was then studied with all known mammalian phosphoinositides. PtdIns(3,4,5)P_3 also showed substantial binding, whereas PtdIns, PtdIns3P, PtdIns4P, PtdIns5P, PtdIns(3,4)P_2, and PtdIns(3,5)P_2 exhibited far lower affinities (Fig. 1D). No binding was observed of other acidic phospholipids, such as phosphatidic acid and phosphatidylserine (Fig. 1D). We also carried out liposome binding assays for the AP180 ENTH domain. AP180 ENTH bound to PtdIns(4,5)P_2 strongly and also showed a lower affinity for PtdIns(3,4,5)P_3 (Fig. 1E).

[1]Department of Biochemistry, Institute of Medical Science, University of Tokyo, 4-6-1 Shirokanedai, Minato-ku, Tokyo 108-8639, Japan. [2]RIKEN Genomic Sciences Center, 1-7-22 Suehiro-cho, Tsurumi-ku, Yokohama-shi, Kanagawa 230-0045, Japan. [3]Cellular Signaling Laboratory, RIKEN Harima Institute at SPring-8, 1-1-1 Kouto, Mikazuki-cho, Sayo, Hyogo 679-5148, Japan. [4]Department of Biochemistry, Hiroshima University School of Medicine, 1-2-3 Kasumi, Minami-ku, Hiroshima 734–8551, Japan. [5]Department of Biophysics and Biochemistry, Graduate School of Science, University of Tokyo, 7-3-1 Hongo, Bunkyo-ku, Tokyo 113-0033, Japan.

*To whom correspondence should be addressed. E-mail: takenawa@ims.u-tokyo.ac.jp

Thus, the ENTH domain is an evolutionally conserved unit designed for strong binding to PtdIns(4,5)P_2.

We next studied intracellular localization of the epsin ENTH domain using green fluorescent protein (GFP) fusion proteins (*10*). COS-7 cells transfected with the GFP-pleckstrin homology (PH) domain of phospholipase C–δ1 (PLC-δ1) showed localization at the plasma membrane (*11*, *12*), whereas GFP alone showed no specific localization. Transfected GFP-epsin ENTH domain was also localized to the plasma membrane, even after the treatment with 300 nM wortmannin [Web fig. 1 (*10*)], indicating an interaction with the plasma membrane, presumably via PtdIns(4,5)P_2 but not through PtdIns(3,4,5)P_3 in vivo.

To identify the phosphoinositide binding site of the epsin ENTH domain, we investigated the interaction of the epsin ENTH domain with inositol-1,4,5-trisphosphate [Ins(1,4,5)P_3], the head group of PtdIns(4,5)P_2, using nuclear magnetic resonance (NMR) spectroscopy. Changes in the backbone amide ^{1}H and ^{15}N chemical shifts of the epsin ENTH domain were measured as a function of Ins(1,4,5)P_3 concentration (Fig. 2A). Mapping of the changes in the chemical shift onto the three-dimensional structure showed that the most perturbed residues are localized at three sites: the NH_2-terminal unstructured region (site 1), the solvent-exposed surface of the first helix (site 2), and the region around loop 1 (loop connecting helices 1 and 2) and loop 3 (loop connecting helices 3 and 4) and helix 4 (site 3) (Fig. 2, A and B). Calculation of the electrostatic surface potential of the epsin ENTH domain showed that sites 1 and 3 are positively charged, whereas site 2 is negatively charged (Fig. 2C). In addition, highly conserved residues in ENTH domains were concentrated at site 3 (Arg^{63}, Trp^{71}, Arg^{72}, and Lys^{76}) (Fig. 2D). To evaluate the importance of these sites, several residues were mutated, and the binding affinities for PtdIns(4,5)P_2 were studied (Fig. 2, E and F).

Substitution of alanine for Arg^{63} and Lys^{76} almost completely abolished PtdIns(4,5)P_2 binding of the epsin ENTH domain, whereas substitution for Arg^{72} only slightly decreased the affinity. Substitution for Lys^{86}, which is located at the end of helix 4 but is distant from site 3, did not affect phosphoinositide binding (Fig. 2E). Thus, specific residues in site 3 appeared to be involved in the direct binding of PtdIns(4,5)P_2.

Many residues in site 1 showed large chemical shift changes, suggesting a large structural change upon phosphoinositide binding (Fig. 2A). Deletion of the entire site 1 region (NH_2-terminal, 18 residues) resulted in a complete loss of PtdIns(4,5)P_2 binding (Fig. 2F). Of the positively charged residues within this region, only Arg^8 was shown to be essential for binding (Fig. 2F). Results suggest that site 1, the NH_2-terminal unstructured region, was necessary for binding and adopted a specific conformation upon binding to PtdIns(4,5)P_2.

The most probable binding model, based on these data, is as follows: the head moiety of PtdIns(4,5)P_2 binds to the cleft composed of loop 1, helix 3, and helix 4. Subsequently, the NH_2-terminal unstructured region binds to site 2, and Arg^8 is positioned near the binding site. The side chains of three basic residues (Arg^8, Arg^{63}, and Lys^{76}) then form salt bridges with the phosphate groups of PtdIns(4,5)P_2 (Fig. 2G).

In addition to the ENTH domain, epsin contains several motifs involved in linking clathrin-coat proteins such as AP-2, Eps15, and clathrin heavy chain (*2*, *13*). The interactions with these proteins are mediated by Asp-Pro-Trp (DPW), Asn-Pro-Phe (NPF), and clathrin-binding motifs present in the central to COOH-terminal region of the epsin molecule (Fig. 3A). Overexpression of epsin DPW motifs results in an inhibition of clathrin-mediated endocytosis (*2*).

To evaluate the importance of the interaction between the ENTH domain and phosphoinositide in endocytosis in vivo, we studied the effect of mutant epsin overexpression on endocytosis in COS-7 cells. COS-7 cells treated with Texas Red–conjugated epidermal growth factor (EGF) showed internalization within 10 min. EGF internalization was not affected by overexpression of wild-type epsin in COS-7 cells (Fig. 3B). In contrast, overexpression of epsin ΔENTH in which the NH_2-terminal ENTH domain was deleted inhibited internalization (Fig. 3, B and C). This inhibition occurred in a competitive manner in which coat proteins such as AP-2 and Eps15 were presumably sequestered by DPW or NPF motifs present in the COOH-terminal half of the mutant epsin molecule overexpressed in the cell. EGF internalization was also inhibited by overexpression of epsin $Lys^{76} \rightarrow Ala^{76}$ (K76A) (Fig. 3, B and C), in which Lys^{76} of the ENTH domain was substituted with an alanine residue. Overexpression of epsin $Arg^{72} \rightarrow Ala^{72}$ (R72A), which still binds to PtdIns(4,5)P_2 (Fig. 2E), did not show any inhibitory effect on EGF internalization (Fig. 3, B and C). Thus, the phosphoinositide-binding ability of the ENTH domain was essential for epsin to induce clathrin-mediated endocytosis, and the lack of this ability was comparable to a loss of the entire ENTH domain.

The epsin ENTH domain associates with a transcription factor, promyelocytic leuke-

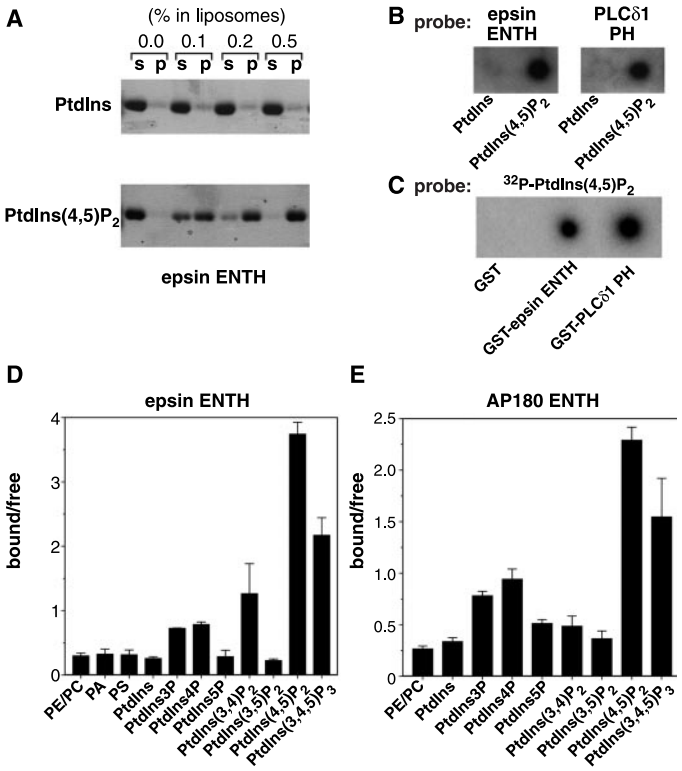

Fig. 1. Specific binding of the ENTH domain to PtdIns(4,5)P_2. (**A**) Co-sedimentation assay with GST-epsin ENTH domain. Liposomes (PE/PC = 4/1; total, 100 μg) containing the indicated ratio (weight %) of phosphoinositides were mixed with 5 μg of GST-ENTH (*24*) and co-sedimented. Proteins in supernatant (s) and precipitate (p) were visualized by SDS–polyacrylamide gel electrophoresis and stained with Coomassie brilliant blue (*25*). (**B**) Overlay assay using protein probe against lipids. GST fusion proteins were labeled with ^{32}P by protein kinase A and overlaid (0.5 μg/ml) against phospholipids (4 μg) blotted onto nitrocellulose membrane (*26*). (**C**) Overlay assay using lipid probe against proteins. [^{32}P]PtdIns(4,5)P_2 was produced by phosphorylation of PtdIns4P with PtdIns4P 5-kinase α and [γ-^{32}P]adenosine 5′-triphosphate as described previously (*27*) and was used as a probe (1×10^6 cpm/ml) against GST fusion proteins (0.1 μg) on nitrocellulose membrane (*28*). Quantitative representations of co-sedimentation assay data of GST-ENTH domains from (**D**) epsin and (**E**) AP180 (*24*) with 0.5% of the indicated phospholipids in the liposomes. Results from three independent experiments are represented as mean values ± SEM (error bars).

mia Zn^{2+} finger protein (PLZF) (*14*), and epsin ENTH R72A fails to bind PLZF. In our study, ENTH R72A still bound to PtdIns(4,5)P_2 (Fig. 2E), and overexpression of epsin R72A did not inhibit EGF internalization (Fig. 3, B and C), suggesting that clathrin-mediated endocytosis does not require an interaction between the ENTH domain and PLZF.

Thus, interaction between PtdIns(4,5)P_2 and the ENTH domain of epsin is indispensable for EGF internalization mediated by clathrin-coated pits. Internalization of insulin into CHO-IR cells is inhibited by overexpression of the epsin ENTH domain (*15*), which may indicate a competitive inhibition of ENTH-phosphoinositide binding. All known proteins carrying ENTH domains, such as epsin, AP180, and Hip1R (Sla2p), have been reported to bind clathrin and AP-2 directly or to colocalize with clathrin-coated pits (*2*, *4*, *16*, *17*). This family of proteins is thought to play a regulatory role in the formation of coated pits, invagination of the plasma membrane, or the formation of coated vesicles (*2*,

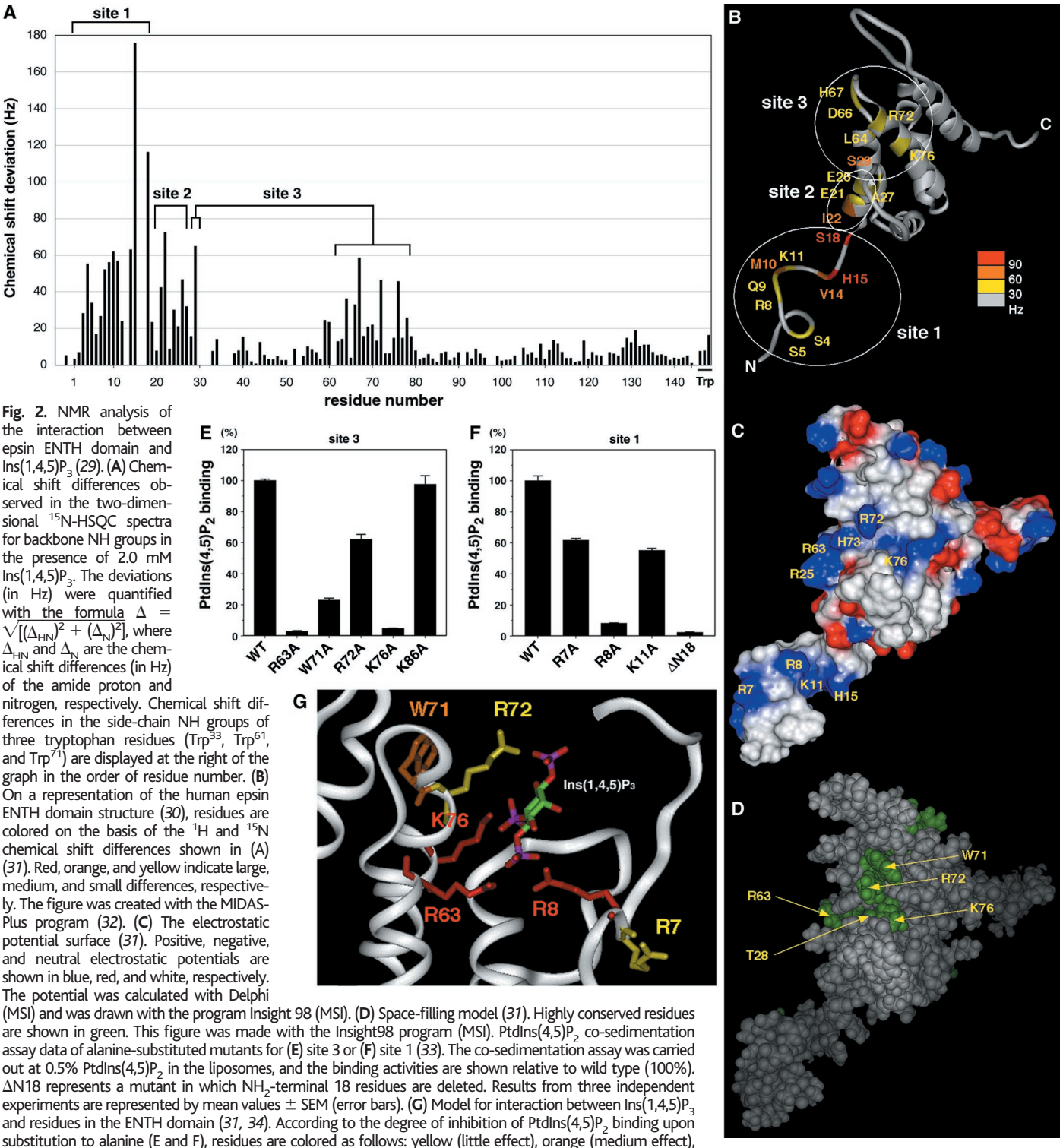

Fig. 2. NMR analysis of the interaction between epsin ENTH domain and Ins(1,4,5)P_3 (*29*). (**A**) Chemical shift differences observed in the two-dimensional ^{15}N-HSQC spectra for backbone NH groups in the presence of 2.0 mM Ins(1,4,5)P_3. The deviations (in Hz) were quantified with the formula $\Delta = \sqrt{[(\Delta_{HN})^2 + (\Delta_N)^2]}$, where Δ_{HN} and Δ_N are the chemical shift differences (in Hz) of the amide proton and nitrogen, respectively. Chemical shift differences in the side-chain NH groups of three tryptophan residues (Trp^{33}, Trp^{61}, and Trp^{71}) are displayed at the right of the graph in the order of residue number. (**B**) On a representation of the human epsin ENTH domain structure (*30*), residues are colored on the basis of the ^{1}H and ^{15}N chemical shift differences shown in (A) (*31*). Red, orange, and yellow indicate large, medium, and small differences, respectively. The figure was created with the MIDAS-Plus program (*32*). (**C**) The electrostatic potential surface (*31*). Positive, negative, and neutral electrostatic potentials are shown in blue, red, and white, respectively. The potential was calculated with Delphi (MSI) and was drawn with the program Insight 98 (MSI). (**D**) Space-filling model (*31*). Highly conserved residues are shown in green. This figure was made with the Insight98 program (MSI). PtdIns(4,5)P_2 co-sedimentation assay data of alanine-substituted mutants for (**E**) site 3 or (**F**) site 1 (*33*). The co-sedimentation assay was carried out at 0.5% PtdIns(4,5)P_2 in the liposomes, and the binding activities are shown relative to wild type (100%). ΔN18 represents a mutant in which NH_2-terminal 18 residues are deleted. Results from three independent experiments are represented by mean values ± SEM (error bars). (**G**) Model for interaction between Ins(1,4,5)P_3 and residues in the ENTH domain (*31*, *34*). According to the degree of inhibition of PtdIns(4,5)P_2 binding upon substitution to alanine (E and F), residues are colored as follows: yellow (little effect), orange (medium effect), and red [abolition of PtdIns(4,5)P_2 binding].

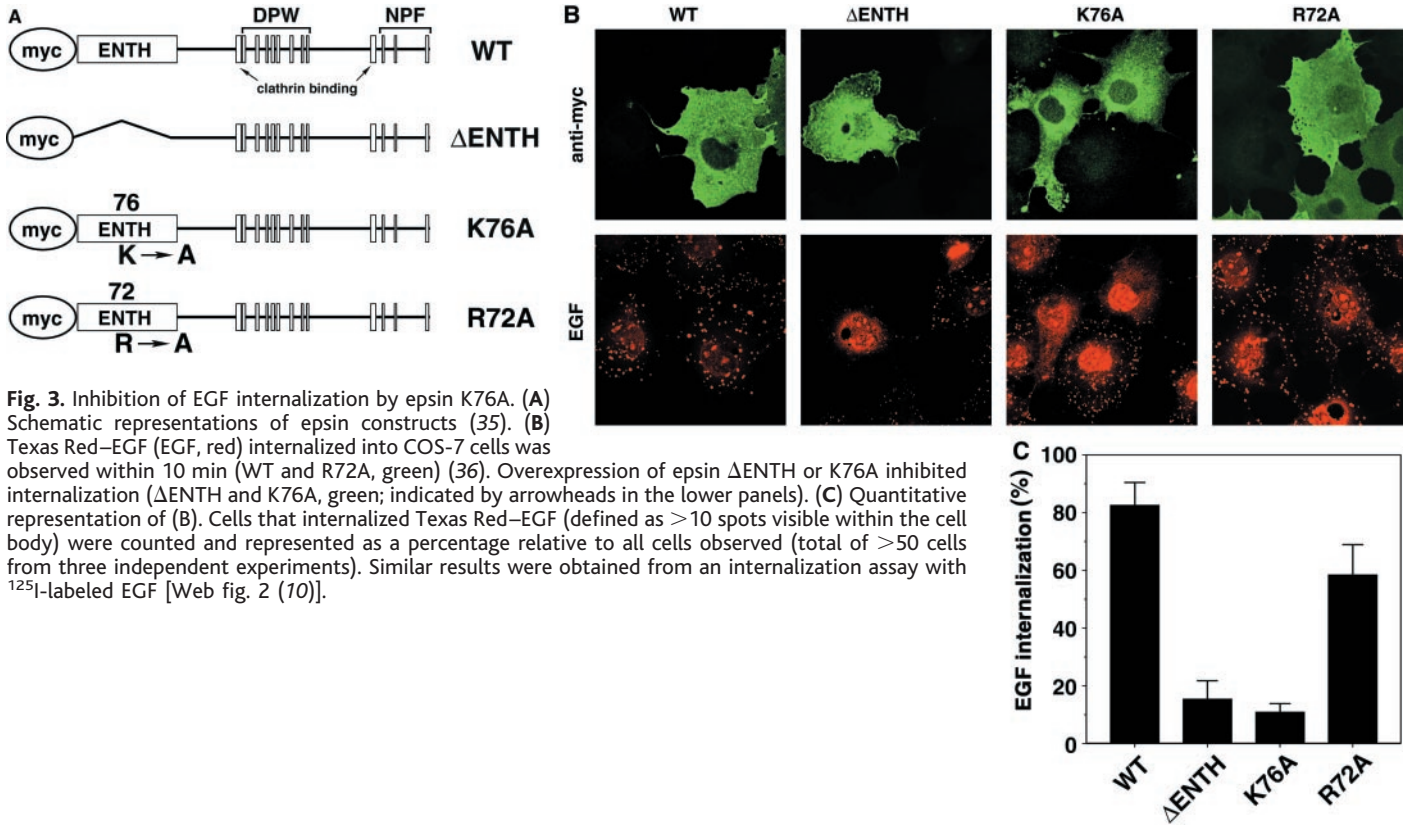

Fig. 3. Inhibition of EGF internalization by epsin K76A. (**A**) Schematic representations of epsin constructs (*35*). (**B**) Texas Red–EGF (EGF, red) internalized into COS-7 cells was observed within 10 min (WT and R72A, green) (*36*). Overexpression of epsin ΔENTH or K76A inhibited internalization (ΔENTH and K76A, green; indicated by arrowheads in the lower panels). (**C**) Quantitative representation of (B). Cells that internalized Texas Red–EGF (defined as >10 spots visible within the cell body) were counted and represented as a percentage relative to all cells observed (total of >50 cells from three independent experiments). Similar results were obtained from an internalization assay with ^{125}I-labeled EGF [Web fig. 2 (*10*)].

6, *18*). In this process, ENTH domains may regulate the linkage of the clathrin triskelion to the plasma membrane through phosphoinositides [Web fig. 3 (*10*)]. Phosphoinositide-metabolizing enzymes like synaptojanin may modify these ENTH-membrane interactions (*9*, *19*).

References and Notes

1. B. K. Kay, M. Yamabhai, B. Wendland, S. D. Emr, *Protein Sci.* **8**, 435 (1999).
2. H. Chen *et al.*, *Nature* **394**, 793 (1998).
3. B. Wendland, K. E. Steece, S. D. Emr, *EMBO J.* **18**, 4383 (1999).
4. A. E. Engqvist-Goldstein, M. M. Kessels, V. S. Chopra, M. R. Hayden, D. G. Drubin, *J. Cell Biol.* **147**, 1503 (1999).
5. O. Cremona , P. De Camilli, *Curr. Opin. Neurobiol.* **7**, 323 (1997).
6. T. Kirchhausen, *Annu. Rev. Cell Dev. Biol.* **15**, 705 (1999).
7. P. De Camilli, S. D. Emr, P. S. McPherson, P. Novick, *Science* **271**, 1533 (1996).
8. M. Jost, F. Simpson, J. M. Kavran, M. A. Lemmon, S. L. Schmid, *Curr. Biol.* **8**, 1399 (1998).
9. O. Cremona *et al.*, *Cell* **99**, 179 (1999).
10. Supplemental figures are available at www.sciencemag.org/cgi/content/full/291/5506/1047/DC1.
11. P. Varnai, T. Balla, *J. Cell Biol.* **143**, 501 (1998).
12. K. Hirose, S. Kadowaki, M. Tanabe, H. Takeshima, M. Iino, *Science* **284**, 1527 (1999).
13. M. T. Drake, M. A. Downs, L. M. Traub, *J. Biol. Chem.* **275**, 6479 (2000).
14. J. Hyman, H. Chen, P. P. Di Fiore, P. De Camilli, A. T. Brunger, *J. Cell Biol.* **149**, 537 (2000).
15. S. Nakashima *et al.*, *EMBO J.* **18**, 3629 (1999).
16. W. Hao, Z. Luo, L. Zheng, K. Prasad, E. M. Lafer, *J. Biol. Chem.* **274**, 22785 (1999).
17. W. Ye, E. M. Lafer, *J. Biol. Chem.* **270**, 10933 (1995).
18. B. Zhang *et al.*, *Neuron* **21**, 1465 (1998).
19. C. Haffner, G. Di Paolo, J. A. Rosenthal, P. De Camilli, *Curr. Biol.* **10**, 471 (2000).
20. K. Nagano *et al.*, *J. Biol. Chem.* **274**, 2872 (1999).
21. F. Delaglio *et al.*, *J. Biomol. NMR* **6**, 277 (1995).
22. B. A. Johnson, R. A. Blevins, *J. Biomol. NMR* **4**, 603 (1994).
23. A. T. Brünger, *X-PLOR (Version 3.1): A System for X-ray Crystallography and NMR* (Yale Univ. Press, New Haven, CT, 1993).
24. cDNA corresponding to the ENTH domain of rat epsin (amino acids 1 through 162) was obtained by reverse transcriptase–polymerase chain reaction (RT-PCR) with the following primers: 5′-CGGGATCCATGTCGACATCATCGCTGCGG-3′ and 5′-CGGGATCCGGAAGCCGTGGCAGTCTGTG-3′. The ENTH domain of rat AP180 (amino acids 1 through 170) was amplified with 5′-CGGAATTCATGTCGGGCCAAACGCTCAC-3′ and 5′-CGGAATTCGATTGGCATGCTCTTCAGCAAC-3′. The obtained cDNA sequences were verified and subcloned into the Bam HI (epsin ENTH) or Eco RI (AP180 ENTH) site of the pGEX4T-3 vector (Amersham Pharmacia Biotech). Construction of GST–PLC-δ1 PH was as described previously (*20*). GFP-ENTH expression vectors were constructed by ligation of the corresponding cDNA into the Bam HI site of pEGFP-C1 (Clontech).
25. V. Patki *et al.*, *Proc. Natl. Acad. Sci. U.S.A.* **94**, 7326 (1997).
26. J. M. Kavran *et al.*, *J. Biol. Chem.* **273**, 30497 (1998).
27. T. Itoh, H. Ishihara, Y. Shibasaki, Y. Oka, T. Takenawa, *J. Biol. Chem.* **275**, 19389 (2000)
28. J. K. Klarlund *et al.*, *Science* **275**, 1927 (1997).
29. Titration experiments with the human epsin ENTH domain (amino acids 1 through 144) and Ins(1,4,5)P_3 were performed at 303 K on a Bruker DRX500 spectrometer in the presence of 0.4 mM of ^{15}N-labeled epsin ENTH domain in 90% H_2O/10% ^2H_2O buffer containing 20 mM sodium phosphate (pH 6.5), 200 mM NaCl, 2 mM $^2H_{10}$ dithiothreitol, and 0.01% sodium azide. In the construct used for these experiments, four residues (Gly, Ser, Ser, and Arg) derived from the expression vector were added to the NH_2-terminus of the epsin ENTH domain. Ins(1,4,5)P_3 was dissolved in the same buffer as the protein sample and was added to the sample. The two-dimensional ^{1}H-^{15}N heteronuclear single-quantum coherence (HSQC) spectra were acquired at Ins(1,4,5)P_3 concentrations of 0, 0.04, 0.1, 0.2, 0.4, 0.8, 1.2, 2.0, and 4.0 mM. All spectra were processed with the program NMRPipe (*21*). Analysis of the processed data was performed with NMRView software (*22*).
30. S. Koshiba, T. Kigawa, A. Kikuchi, S. Yokoyama, *J. Struct. Funct. Genomics*, in press.
31. Single-letter abbreviations for the amino acid residues are as follows: A, Ala; D, Asp; E, Glu; H, His; I, Ile; K, Lys; L, Leu; M, Met; Q, Gln; R, Arg; S, Ser; T, Thr; V, Val; and W, Trp.
32. T. E. Ferrin, C. C. Huang, L. E. Jarvis, R. Langridge, *J. Mol. Graphics* **6**, 13 (1988).
33. Site-directed mutagenesis was carried out by PCR with mutated primers. Fragments upstream and downstream from the mutated sites were amplified independently, mixed together, and used as template for further PCR to obtain the entire region.
34. Model of the interaction of the ENTH domain with Ins(1,4,5)P_3. The NH_2-terminal unstructured region (residues 1 through 18) was oriented near the first helix, and Ins(1,4,5)P_3 was then modeled in the binding site to avoid steric clashes. The orientation of the Lys^{76} side chain was altered toward the phosphate group of Ins(1,4,5)P_3. Modeling was performed with the program Insight98 (MSI, San Diego, CA). Energy minimization was performed with the program X-PLOR 3.1 (*23*).
35. Full-length rat epsin cDNA was obtained in three parts (amino acids 1 through 233, 234 through 323, and 324 through 575) by RT-PCR with the following primers: 5′-CCGCTCGAGATGTCGACATCATCGCTGCGG-3′, 5′-CATCCCCACGACGGATCCG-3′, 5′-GAAGAGCGGATCCGTCGTGG-3′, 5′-CCTCCAAGGATCCCCGGAG-3′, 5′-CTCCGGGGATCCTTGGAGG-3′, and 5′-GCTCTAGATTATAGGAGGAAGGGGTTAG-3′. After the sequences were verified, three fragments were ligated via Xho I–Bam HI, Bam HI–Bam HI, and Bam HI–Xba I sites and then inserted into the Sal I–Xba I site of the pCMV-myc vector. For production of epsin ΔENTH, a Pst I–Xba I fragment corresponding to amino acids 238 through 575 was ligated into pCMV-myc.
36. An EGF internalization assay was carried out 48

hours after transfection. COS-7 cells were incubated with EGF (0.1 μg/ml) [biotinylated, complexed to Texas Red–streptoavidin (Molecular Probes, Eugene, OR)] in binding buffer [20 mM Hepes–NaOH (pH 7.5), 130 mM NaCl, and 0.1% bovine serum albumin] at 4°C for 60 min. Internalization of EGF was allowed by incubation in Dulbecco's modified Eagle's medium at 37°C for 10 min, then excess EGF was removed with 0.2 M AcOH (pH 2.5) and 0.5 M NaCl at 4°C for 5 min. Cells were fixed in 3.7% formaldehyde, permeabilized with 0.2% Triton X-100, and immunostained with a polyclonal antibody to myc (Santa Cruz Biotechnology, Santa Cruz, CA) and fluorescein isothiocyanate–conjugated antibody to rabbit (Organon Teknika, Boxtel, Netherlands). Internalization of EGF was observed by confocal microscopy (Bio-Rad).

37. We thank Y. Watanabe (Ehime University, Japan) for providing us with various synthetic phosphoinositides.

16 October 2000; accepted 15 December 2000

Simultaneous Binding of PtdIns(4,5)P_2 and Clathrin by AP180 in the Nucleation of Clathrin Lattices on Membranes

Marijn G. J. Ford, Barbara M. F. Pearse, Matthew K. Higgins, Yvonne Vallis, David J. Owen, Adele Gibson,* Colin R. Hopkins,* Philip R. Evans,† Harvey T. McMahon†

Adaptor protein 180 (AP180) and its homolog, clathrin assembly lymphoid myeloid leukemia protein (CALM), are closely related proteins that play important roles in clathrin-mediated endocytosis. Here, we present the structure of the NH_2-terminal domain of CALM bound to phosphatidylinositol-4,5-bisphosphate [PtdIns(4,5)P_2] via a lysine-rich motif. This motif is found in other proteins predicted to have domains of similar structure (for example, Huntingtin interacting protein 1). The structure is in part similar to the epsin NH_2-terminal (ENTH) domain, but epsin lacks the PtdIns(4,5)P_2-binding site. Because AP180 could bind to PtdIns(4,5)P_2 and clathrin simultaneously, it may serve to tether clathrin to the membrane. This was shown by using purified components and a budding assay on preformed lipid monolayers. In the presence of AP180, clathrin lattices formed on the monolayer. When AP2 was also present, coated pits were formed.

Budding of clathrin-coated vesicles is a process by which cells package specific cargo into vesicles in a regulated fashion (*1*–*3*). Important functions are the uptake of nutrients, the regulation of receptor and transporter numbers on the plasma membrane, and the recycling of synaptic vesicles. AP180 and AP2 are both major components of clathrin coats. AP2 is a heterotetrameric complex that binds to phosphoinositides in the membrane and to the cytoplasmic domains of membrane proteins destined for internalization (*1*, *3*, *4*). AP2 binds clathrin and can stimulate clathrin cage assembly in vitro (*5*, *6*). It also interacts with a range of cytoplasmic proteins including AP180 (*7*). Like AP2, AP180 also binds directly to clathrin and can stimulate clathrin cage assembly in vitro, limiting the size distribution of the resulting cages (*8*–*11*). The related proteins, CALM (AP180-2, a close homolog of synaptic AP180), LAP (the *Drosophila* AP180 homolog), and UNC-11 (the *Caenorhabditis elegans* homolog), are all implicated in clathrin-coated vesicle endocytosis (*12*, *13*). CALM was identified and named because of its homology to AP180 and to reflect its involvement in t(10;11) chromosomal translocations found in various leukemias (*14*). Disruptions of the *LAP* and *Unc-11* genes impair clathrin-dependent recycling of synaptic vesicles, resulting in fewer vesicles of more variable size. The NH_2-terminal domain of AP180 (AP180-N) shows the highest degree of conservation across AP180 homologs, and binds to inositol polyphosphates (*10*, *15*, *16*), whereas the COOH-terminal domain contains the putative clathrin- and AP2-binding sites (Fig. 1A).

When expressed in COS-7 fibroblasts, both full-length AP180 and AP180-C (residues 530 to 915) inhibited uptake of epidermal growth factor (EGF) and transferrin (*17*) (Fig. 1B), as is the case for CALM (*18*). Clathrin was redistributed in transfected cells, and we noted fewer coated pits per unit of cell surface–membrane length (8% of control, Fig. 1C). This showed that endocytosis was inhibited by blocking clathrin-coated pit formation, consistent with the ability of the COOH-terminus to bind clathrin and to stimulate cage assembly in vitro (*8*–*11*). However, AP180-N overexpression did not inhibit EGF or transferrin uptake (Fig. 1B). It had no apparent protein-binding partners but is more localized to the plasma membrane, consistent with binding to polyphosphoinositides (*15*, *16*).

To probe the molecular basis of phosphoinositide interactions, we solved the structure of the NH_2-terminal domain from the close AP180 homolog, CALM, at 2 Å resolution (*19*, *20*) (crystals of AP180-N did not diffract well). There were nine α helices forming a solenoid structure (Fig. 2). This is reminiscent of other protein families formed from a superhelix of α helices such as the armadillo (*21*) and tetratricopeptide repeat (*22*) domains, but it is most similar to the ENTH domain of epsin (*23*) (Fig. 2B). The first seven helices of epsin superimposed well on those of CALM. In epsin, however, the final α8 helix folded back across the others, whereas in CALM the final three long helices continued the solenoidal pattern. Because of the high sequence homology of CALM-N and AP180-N (81% sequence identity) (Fig. 2), we can safely assume that the NH_2-terminal domain of AP180 has the same structure.

X-ray data were collected at 2 Å resolution from CALM-N crystals soaked in a series of inositol phosphates and phospholipids. Binding was observed for inositol hexakisphosphate (D-*myo*-inositol-1,2,3,4,5,6-hexakisphosphate, $InsP_6$), inositol-4,5-bisphosphate [Ins(4,5)P_2], and a soluble short-chain (diC_8) L-α-D-*myo*-phosphatidylinositol-4,5-bisphosphate. No significant binding was observed in the crystal for short-chain (diC_8) L-α-D-*myo*-phosphatidylinositol-3,4,5-trisphosphate. The binding site is unusual (Fig. 2): Typical ligand-binding sites on proteins lie in a pocket or groove, but this site is on the surface, with the phosphates perched on the tips of the side chains of three lysines and a histidine, like a ball balanced on the fingertips. In all ligands, only the two phosphates were well ordered and contacted the protein. The cluster of lysines and histidine formed a marked positively charged patch on the surface (Fig. 2C), appropriate for a phosphate-binding protein.

Database searches with the AP180-N/CALM-N identified several classes of related sequences (Fig. 2H). First, there were the members of the AP180 family itself, with a conserved NH_2-terminal domain, having PtdIns(4,5)P_2-binding motifs, which we identified from the observed binding in the crystal, $K(X)_9KX(K/R)(H/Y)$. The COOH-terminal domains of these proteins contain clathrin-binding motifs (*3*, *24*), as well as Asp-Pro-Phe (DPF)-like α- and β-adaptin–

Medical Research Council (MRC) Laboratory of Molecular Biology, Hills Road, Cambridge, CB2 2QH, UK.

*MRC Laboratory of Molecular and Cell Biology, University College London, Gower Street, London, WC1E 6BT, UK.

†To whom correspondence should be addressed. E-mail: pre@mrc-lmb.cam.ac.uk, hmm@mrc-lmb.cam.ac.uk